



**Discover Generics**  
Cost-Effective CT & MRI Contrast Agents

 FRESENIUS  
KABI

**WATCH VIDEO**

## Errata

# AJNR

*AJNR Am J Neuroradiol* 1994, 15 (6) A9-A10  
<http://www.ajnr.org/content/15/6/A9.citation>

This information is current as  
of June 1, 2025.

## Errata

Several references published in the paper "Congenital Defects of the Posterior Arch of the Atlas: A Report of Seven Cases Including an Affected Mother and Son" by Guido Currarino, Nancy Rollins, and Jan T. Diehl, which appeared on pages 249–254 of the February 1994 issue of the *AJNR*, were incorrect because of an error made by the printer. The references were submitted correctly by the author. The references are listed correctly below. The printer regrets the error.

## References

14. Brocher JE. Konstitutionell bedingte Veränderungen des Wirbelogen. *Fortschr Röntgenstr* 1960;92:363–380
15. Holsten DR. Eine besondere Form von Defektbildung in hintere Atlasbogen. *Fortschr Röntgenstr* 1968;108:541–543
16. Keller HL. Formvarianten und Fehlbildung des Atlas und seiner Umgebung. *Fortschr Röntgenstr* 1961;95:361–370
19. Seibert FM. Irrtümer bei angeborene und unfallbedingten Wirbelsäulenveränderungen. *Fortschr Röntgenstr* 1950;73:464–470
22. Becker HW. Beitrag zur Aplasie des hinteren Atlasbogens. *Fortschr Röntgenstr* 1964;101:204–206
25. Gockel HP. Über eine Form von Atlasfehlfbildung. *Fortschr Röntgenstr* 1958;88:485–487
27. Pöschl M. Hemmungsmissbildung am Bogenteil der oberen Halswirbel. *Fortschr Röntgenstr* 1943;67:138–143

Figures 2 (A–D) and Figures 4 (A–D) were inadvertently switched by the printer in the article "MR Imaging of the Middle Cerebral Artery Stenosis and Occlusion: Value of MR Angiography," by Norihiko Fujita, Norio Hirabuki, Keiko Fujii, Tsutomu Hashimoto, Takashi Miura, Tadayuki Sato, and Takahiro Kozuka, published on pages 335–341 of the February 1994 issue. The correct figures, as they should have appeared, are shown below. The printer regrets the error.

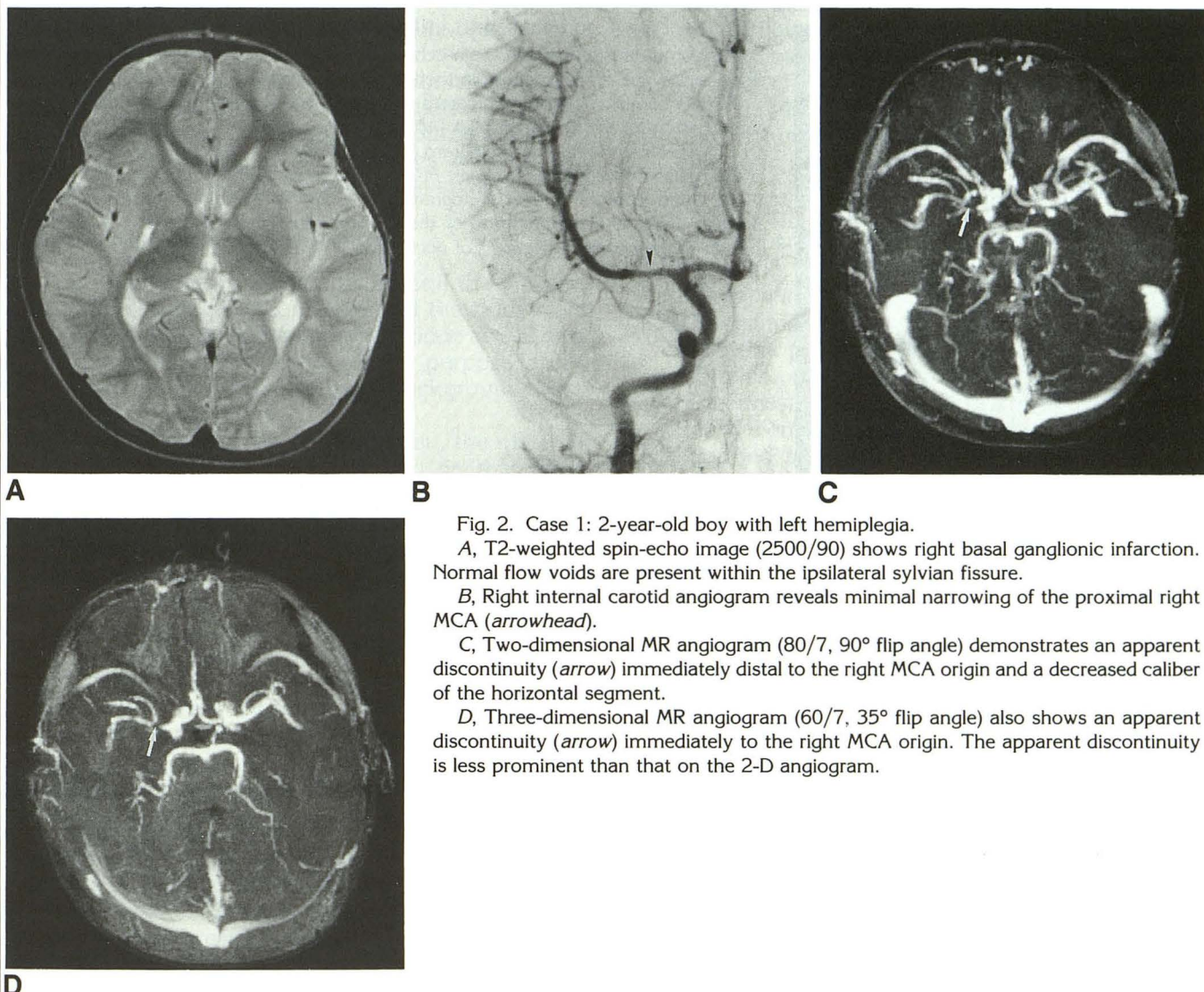


Fig. 2. Case 1: 2-year-old boy with left hemiplegia.

*A*, T2-weighted spin-echo image (2500/90) shows right basal ganglionic infarction. Normal flow voids are present within the ipsilateral sylvian fissure.

*B*, Right internal carotid angiogram reveals minimal narrowing of the proximal right MCA (arrowhead).

*C*, Two-dimensional MR angiogram (80/7, 90° flip angle) demonstrates an apparent discontinuity (arrow) immediately distal to the right MCA origin and a decreased caliber of the horizontal segment.

*D*, Three-dimensional MR angiogram (60/7, 35° flip angle) also shows an apparent discontinuity (arrow) immediately to the right MCA origin. The apparent discontinuity is less prominent than that on the 2-D angiogram.

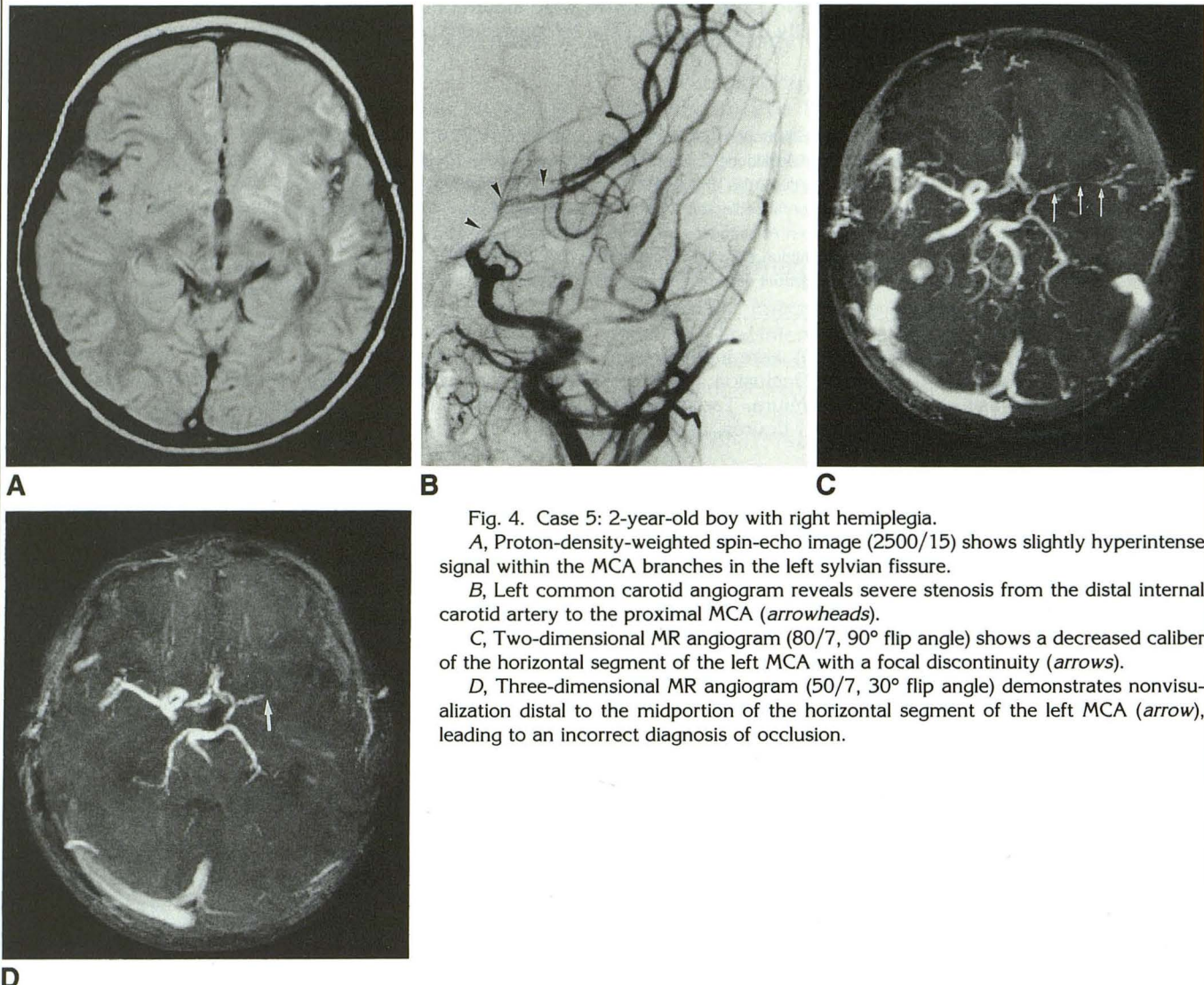


Fig. 4. Case 5: 2-year-old boy with right hemiplegia.

A, Proton-density-weighted spin-echo image (2500/15) shows slightly hyperintense signal within the MCA branches in the left sylvian fissure.

B, Left common carotid angiogram reveals severe stenosis from the distal internal carotid artery to the proximal MCA (arrowheads).

C, Two-dimensional MR angiogram (80/7, 90° flip angle) shows a decreased caliber of the horizontal segment of the left MCA with a focal discontinuity (arrows).

D, Three-dimensional MR angiogram (50/7, 30° flip angle) demonstrates nonvisualization distal to the midportion of the horizontal segment of the left MCA (arrow), leading to an incorrect diagnosis of occlusion.